Separation and Purification Technology 317 (2023) 123798

Contents lists available at ScienceDirect

Separation and Purification Technology

journal homepage: www.elsevier.com/locate/seppur

Ion exchange resin – Bipolar membrane electrodialysis hybrid process for reverse osmosis permeate remineralization: Cation exchange resins equilibria and kinetics

A.A.M. Abusultan [a], J.A. Wood [a], T. Sainio [b], A.J.B. Kemperman [a,*], W.G.J. van der Meer [a,c]

[a] Membrane Science and Technology Cluster, MESA+ Institute for Nanotechnology, Faculty of Science and Technology, University of Twente, P.O. Box 217, NL-7500 AE Enschede, The Netherlands
[b] LUT University, School of Engineering Science, Department of Separation Science, Mukkulankatu 19, 15210 Lahti, Finland
[c] Oasen N.V., P.O. Box 122, 2800 AC Gouda, The Netherlands

ARTICLE INFO

Keywords:
Ion exchange resin
Sorption equilibria
Mass transfer
Chelating resin

ABSTRACT

Reverse osmosis (RO) membrane technology is widely used for producing high-quality drinking water. Yet RO permeate is by itself acidic (pH = 5.5 to 6.0), unbuffered and has low mineral content, therefore post treatment i.e., remineralization is mostly required. An ion exchange resin – bipolar membrane electrodialysis hybrid process was developed for sustainable RO permeate remineralization. Fundamental phenomena in the recovery of calcium and magnesium by ion exchange to remineralize reverse osmosis permeate were investigated. Sorption equilibrium and mass transfer kinetics were investigated for weakly acidic (Amberlite IRC747, Amberlite IRC748, Lewatit S8227) and strongly acidic (DOWEX Marathon MSC) cation exchange resins. Most suitable resin for the remineralization process should have high selectivity for calcium and magnesium and low selectivity for monovalent ions to avoid adding undesired ions to the remineralised water downstream as well as relatively fast mass transfer kinetics. The isotherms were correlated with the stoichiometric ion exchange isotherm and the Langmuir-Freundlich (Sips) isotherm. All resins showed high selectivity for ions with higher valence, but weakly acidic cation exchange (WAC) resins showed significantly lower selectivity towards monovalent ions than the strongly acidic cation exchange resin. The influence of each resin functional group, charge density and degree of protonation was shown to have a major effect on the resin selectivity. Amberlite IRC748 had the lowest selectivity ($K_{NH4+/Na+} = 0.77 \pm 0.19$) and removal (46%) for ammonium in a single-component system. The mass transfer rate was found to be controlled by intraparticle diffusion rather than film diffusion. Amberlite IRC748 is recommended for use in a remineralization process where divalent ions are present because of its favourable sorption and higher mass transfer kinetics ($K_s = 8.65 \pm 0.58 \times 10^{-12}$, $7.95 \pm 0.38 \times 10^{-12}$ m^2/s for calcium and magnesium, respectively).

1. Introduction

The increasing demand for high-quality water, along with limited water resources, motivates the need for innovative and sustainable water purification methods. Reverse osmosis (RO) is considered the leading membrane technology for the production of pure drinking water [1]. RO use has been extended beyond seawater and brackish groundwater desalination to, for example, dairy, pharmaceuticals, textile and dyeing industries, etc. [2]. Paradoxically, reverse osmosis may have created too clean drinking water, which by itself can be harmful to piping distribution networks due to the extremely low mineral content [3]. Therefore, a post-treatment process i.e., remineralization is needed to adjust the water quality in the network.

Remineralization is a post-treatment process wherein mainly calcium and magnesium concentration (water hardness) together with carbonate/bicarbonate alkalinity of RO permeate is adjusted [4]. Remineralization is necessary to safeguard the integrity of the water distribution system and comply with drinking water standards/regulations [5]. Although the European Drinking Water Directive does not mention a limit for water hardness, several EU countries have set regulations by law or technical guidelines for water hardness content [6]. For example, following the Dutch water quality standards (where this

* Corresponding author.
E-mail address: a.j.b.kemperman@utwente.nl (A.J.B. Kemperman).

https://doi.org/10.1016/j.seppur.2023.123798
Received 24 January 2023; Received in revised form 3 April 2023; Accepted 4 April 2023
Available online 6 April 2023

study is carried out), a minimum of 1.0 mM water hardness in water is required [7]. Commonly applied remineralization methods are blending, calcite dissociation and direct dosage of chemicals [8]. While, blending untreated water with RO permeate of remineralization involves less control over the final water quality, calcite dissociation and direct dosage remineralization methods include either frequent change of the calcite material or extra chemical use.

As an alternative approach to the commonly applied remineralization processes, a sorption-membrane process hybrid based on Ion Exchange (IEX) and Bipolar Membrane Electrodialysis has been investigated (Fig. 1) [9]. The process developed aims at the recovery of hardness ions from source water for RO permeate remineralization. First, anaerobic groundwater is fed to a cation exchange resin (CEX) for the selective removal of divalent ions. Second, the softened feed water enriched with singly charged ions enters the RO unit which then can operate at much higher recoveries, due to the absence of scaling-forming ions (calcium and magnesium). Third, RO retentate enriched with singly charged ions is used for producing HCl and NaOH using BMED. Forth, the BMED-produced acid stream (HCl) is used to regenerate the cation exchange resin where the separation of monovalent/divalent ions occurs. Finally, the CEX regenerant is passed through an anion exchange resin (AEX)to avoid adding chloride to the reverse osmosis permeate, by replacing Cl^- with HCO_3^- and producing calcium and magnesium bicarbonate as the final remineralization process products. The ion exchange process is batch and sequential, i.e., the resin loading step is followed by regeneration with the produced acid/base using the BMED process.

In addition to calcium and magnesium, groundwater in the Netherlands typically contains alkali metals (e.g. sodium, potassium) and ammonium, in addition to, heavy metals such as iron and manganese, and traces of heavy metals [10]. Each of these ions would have an impact on the purity of the recovered calcium and magnesium. Other heavy metals are usually present in very low concentrations such as zinc and copper, etc. Iron and manganese are soluble under anaerobic conditions in the Fe^{2+} and Mn^{2+} form, however, under aerobic conditions, they become unstable and form Fe^{3+} and Mn^{3+} hydroxide precipitates. The experiments in this research were done under aerobic conditions since it was impractical to operate under anaerobic conditions and hence the model water composition used was limited to ammonium, potassium, calcium and magnesium ions. In real groundwater, the heavy metal ions could affect the resin selectivity and hence the actual remineralization process.

The effect of calcium and magnesium concentration in drinking water on human health is much debated among researchers. While some of them argue that calcium and magnesium deficiency can increase the rate of several diseases, for instance, cerebrovascular and cardiovascular diseases [11–14], others found no evidence for a significant relationship between water hardness and cardiovascular mortality [15–17]. However, ions in water are often easier to be adsorbed by the human body than when present in food, where they can be bound to other substances. Therefore, a minimum concentration of these elements in drinking water is desirable. A minimum concentration of water hardness of 20 – 30 mg/L should have a positive impact on human health [5,18]. Yet, a more significant reason for maintaining a minimum water hardness in water is to have a buffering capacity to reduce the water network piping deterioration potential [19]. Otherwise, RO permeate will be aggressive to different pipe materials such as copper and asbestos/cement, resulting in the leaching of copper/heavy metals and dissolving of the cement pipes.

On the other hand, the presence of ammonium, as well as high levels of potassium in drinking water, is undesirable. Ammonium can significantly enhance the bacterial growth potential in the water distribution network [20,21]. In addition, increased exposure to potassium could lead to severe problems for people with kidney disease or other issues such as diabetes and heart disease [22]. The Dutch water quality standards set a maximum limitation of 0.2 mg/L ammonium in water. Therefore, ammonium and potassium content in the remineralization stream should be as low as possible to avoid exceeding their limit in the

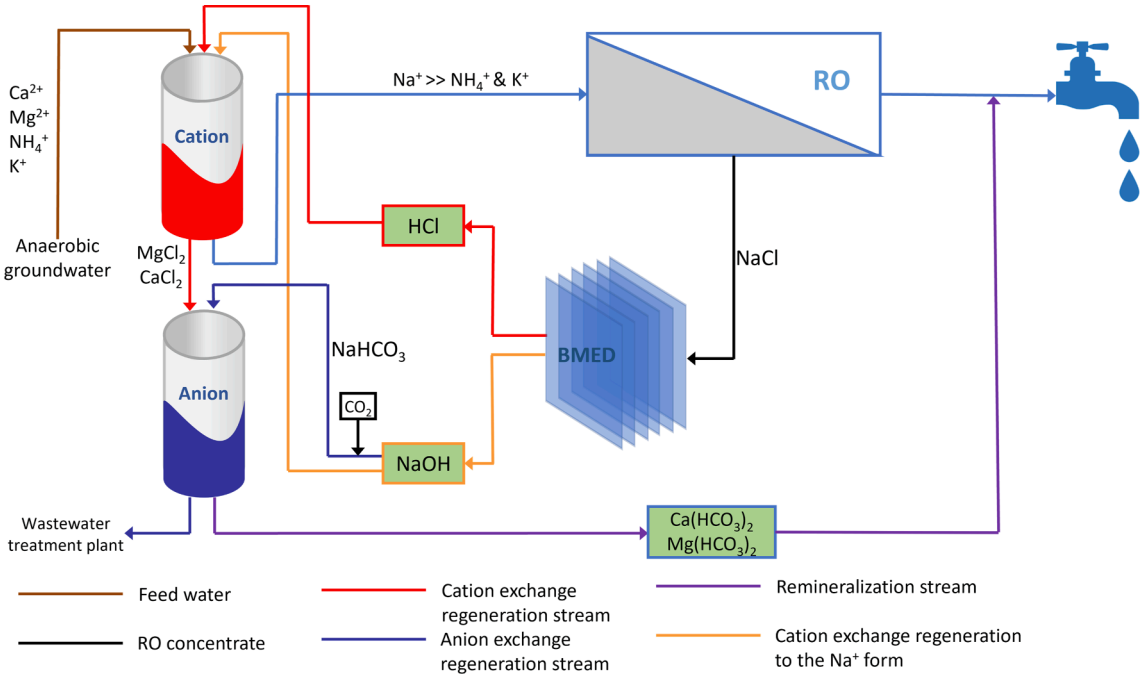

Fig. 1. Reverse osmosis remineralization process scheme based on ion exchange resin and bipolar membrane electrodialysis. A cation exchange resin is used to recover hardness ions from the groundwater to be used for RO permeate remineralization. Anion exchange resin is needed to convert chloride into bicarbonate and hence avoid adding chloride downstream. Simultaneously, bipolar membrane electrodialysis is used to produce the required HCl and NaOH for cation and anion exchange resins regeneration, using RO concentrate rich in NaCl. Both anion and cation exchange processes loading, and regeneration are batch and sequential. (Anaerobic ground water pH (CEX feed) ≅ RO feed = 7.20, pH of BMED produced HCl = 0, pH of BMED produced NaOH = 13, pH of CEX regenerant stream = 0, and AER effluent stream during loading i.e., remineralization stream pH = 6–6.5).

final remineralised water.

Ion exchange principles and materials are applied at analytical, preparative and industrial scale [23]. Ion exchange chromatography is a typical example of using ion exchange for quantitative analysis of ions based on their affinity difference to an ion exchange resin. On the other hand, preparative ion exchange chromatography is meant for the recovery of precious metals and high-value products in high purities, especially in the pharmaceutical industry [24,25]. In water treatment, ion exchange is mainly used for the selective removal of hardness ions in a process called water softening [26]. The use of ion-exchange chromatography principles for large-scale ions recovery in drinking water treatment applications, to the authors knowledge, is yet to be investigated.

Since preparative ion-exchange chromatography is intended for the separation and recovery of compounds in high purities from a stream mixture, a selection of resin material with a high affinity for the desired compound is extremely important. Ion exchange resins are insoluble polymers that contain acidic or basic functional groups. Depending on the solution pH, functional groups are completely (strongly acidic/basic) or partially ionised (weakly acidic/basic). Weakly acidic (WAC) resins are either ordinary (non-chelating) or chelating resins, depending on the functional group ability to form complex bonding with counter-ions. Strongly acidic (SAC) and WAC resins are usually used for the removal of both monovalent and divalent ions, with varying levels of selectivity. SAC resins usually exhibit a higher affinity for monovalent ions compared to WAC resins. WAC ordinary resins are known to have a higher selectivity for divalent ions compared to SAC resins [27]. Moreover, WAC chelating resins are often used in the removal of trace ions and heavy metals [28,29]. Hoffmann and Martinola (1988) [26] showed that WAC chelating resins, especially with iminodiacetic and aminophosphonic groups can be used to efficiently remove calcium from concentrated salt at very low concentrations of 50 ppb Ca^{2+}.

Based on the water quality requirements discussed earlier, the IEX regenerant stream in the investigated remineralization process should have a high content of calcium and magnesium and as low as possible ammonium and potassium content. This is needed to avoid increasing the concentration of the undesired ions such as ammonium and potassium downstream and to reduce the bacterial growth potential enhanced by ammonium presence. On the other hand, the cation resin should be easily regenerated with HCl produced using the bipolar membrane. Moreover, mass transfer kinetics should be fast to enable efficient use of the entire ion exchange column. To comply with this requirement, a cation exchange resin with a high sorption selectivity for Ca^{2+} and Mg^{2+} and a low selectivity for NH_4^+ and K^+, as well as fast mass transfer kinetics is required.

This work does not investigate the complete remineralization process, yet it focuses on investigating the ion exchange equilibria and kinetics of Ca^{2+}, Mg^{2+}, NH_4^+ and K^+ ions on several strongly and weakly acidic (chelating and ordinary) cation exchange resins to select the most promising resin regarding the water quality and the remineralization process requirements. The interplay and trade-off of the complete remineralization process will be investigated in another publication.

2. Materials and methods

2.1. Resins and chemicals

Four commercial cation exchange resins were tested in this study: DOWEX Marathon MSC, Amberlite IRC747 and Amberlite IRC748 were provided by DOW chemicals, the Netherlands, where Lewatit S 8227 was provided by LANXESS, Germany. The physical and chemical properties of the resins shown in Table 1 were measured according to protocols provided by the manufacturer, except for the working pH range which was mentioned in the resins datasheets. DOWEX Marathon MSC and Lewatit S8227 resins were supplied in the H^+ form, while Amberlite IRC747 and IRC748 were supplied in the Na^+ form. All resins were first pre-treated and brought to the Na^+ form for equal comparison. The resins pre-treatment was necessary to remove any remaining impurities from the manufacturing process that could interfere with the sorption experiments. This was in particular the case of Amberlite IRC747&748 resins which have traces of sodium remaining after regeneration to the Na^+ form by the manufacturer. Following the manufacturer's recommendations, the resin pre-treatment was as follows: First of all, the resin material was soaked in Ultra-pure Milli-Q water for 30 min. Then, it was transferred to a glass column provided by GE Healthcare (XK 26/40) whose inlet was adjusted to accommodate 4 mm tubing to operate at flow rates up to 5.0 L/h. After that, 10 bed volumes (BVs) of 2.5 M HCl acid were run through the resin, and later, 20 BVs of 1.0 M NaOH were used to convert the resins into Na^+ form. Finally, the wet resin material was filtered with a 0.45 μm syringe Whatman nylon membrane filter and stored for later use. The resin was rinsed in between with 20 bed volumes of demineralised water to remove the remaining solution of the former step.

Ultra-pure Milli-Q water was used for solution preparation and dilution. Analytical grade ammonium chloride, potassium chloride, calcium chloride dihydrate, magnesium chloride hexahydrate, hydrochloric acid, and sodium hydroxide chemicals were purchased from Merck (former Sigma-Aldrich) (Darmstadt, Germany).

2.2. Analysis of cations

A Metrohm ECO IC ion chromatography device equipped with a C6 cation exchange column was used for the analysis of NH_4^+, K^+, Mg^{2+}, and Ca^{2+} concentration in the collected samples using a 4 mM HNO_3 eluent based on manufacturer recommendations. The pH of the samples and the prepared solutions was measured using a glass electrode (AquaPro 9104APWP, Thermo Fisher Scientific). A Metrohm 805 Dosimat device was used for solution titration.

Table 1
Physical and chemical Characteristics of the resins used in this study. Values reported were measured according to protocols in the references provided except for the pH range which was adopted from the resins manufacturer datasheet.

Ion exchange resin material	DOWEX Marathon MSC	Lewatit S8227	AMBERLITE IRC747	AMBERLITE IRC748
Resin type	Strong	Weak	Weak chelating	Weak chelating
Matrix	Macroporous	Macroporous	Macroporous	Macroporous
Functional group	Sulfonic acid	Carboxylic acid	Aminophosphonic	Iminodiacetic acid
Ionic form as shipped	H^+	H^+	Na^+	Na^+
Total bed capacity [eq/L] [30]	1.78 ± 0.12	3.76 ± 0.01	2.19 ± 0.06	1.42 ± 0.01
Total dry capacity [meqv/g] [30]	5.25 ± 0.35	11.61 ± 0.02	7.12 ± 0.18	4.79 ± 0.03
Total wet capacity [meqv/g] [30]	2.51 ± 0.17	4.26 ± 0.01	2.11 ± 0.05	1.61 ± 0.01
Apparent density [kg/m^3] [31]	1188	1152	1107	1101
Material (Skeletal) density [kg/m^3] [31]	1297 ± 18	1302 ± 12	1203 ± 3	1165 ± 10
Bulk density [kg/m^3] [31]	793.7	793.7	757.6	735.3
Moisture retention capacity [%] [32]	52.20 ± 0.8	63.30 ± 0.1	70.40 ± 0.20	66.40 ± 0.30
Mean particle size (Na^+ form) [μm] [31]	565 ± 1	780 ± 15	581 ± 2	578 ± 5
pH range	0 – 14	5 – 14	5 – 14	5 – 14

2.3. Anaerobic groundwater characterization

Table 2 shows the concentration of the most prevalent cations and anions in a real anaerobic groundwater sample from the Oasen water treatment plant at Kamerik, the Netherlands. A multi-component model solution of similar cation composition and chloride anion was prepared for sorption equilibrium and kinetics experiments. The model solution was tested under aerobic conditions since it was practically difficult to ensure anaerobic conditions in the lab.

2.4. Batch equilibrium experiments

Equilibrium sorption isotherms were obtained by a static method using a solution contains a single electrolyte at a time, using KCl, NH_4Cl, $CaCl_2{\cdot}2H_2O$, and $MgCl_2{\cdot}6H_2O$ analytical grade stock solutions purchased from Merck (former Sigma-Aldrich) (Darmstadt, Germany). The sorption isotherms were obtained using DOWEX Marathon MSC, Lewatit S8227, Amberlite IRC747, and Amberlite IRC748 cation exchange resins initially in Na^+ form. Each experiment was done in triplicate and under aerobic conditions at room temperature (approx. 22 °C). The volume of the solution in each experiment was 100 mL and the solution concentration was 10 meqv/L. The prepared solutions were contacted with varied resin dosing amounts in glass bottles to obtain different data points on the isotherm curve. The resin dose (theoretical removal percentage) is defined as the ratio between the charge equivalents in the resin and the solution (initially) in the batch [33] (Eqn. (2.1)). The resin dose was varied for all resins tested to a factor of 200% in the case of monovalent ions sorption experiment and a factor of 1000% for the divalent ions sorption experiments to achieve a plateau in the removal curve. The actual air-dry resin amount used in each experiment can be back calculated using the resin total wet capacity mentioned in Table 1 according to equation (2.1). Using a magnetic stirrer, the solutions were stirred for 24 h at 180 rpms. After that, samples were collected and filtered using 0.45 μm syringe Whatman nylon membrane filters. Finally, the concentration of each of the ions sorbed by the resin was determined by the difference between its concentrations in the initial solution and at equilibrium, and taking into account the mass of the resin. Moreover, the final solution pH was recorded.

$$Resin\ \ dose\ \ (\%) = \frac{m_d \times q_m}{V \times C_0 \times z_i} \times 100 \tag{2.1}$$

where m_d is the resin dry mass (g), V is the solution volume (L),q_m is the resin dry capacity (meqv/g), C_0 is the initial solution concentration (mmol/L) and z_i is the ionic valence.

The sorption data were fitted using the mass action law which is suitable for homogenous surfaces and by Langmuir-Freundlich (also known as Sips model) model which is more suitable for heterogeneous surfaces [34]. Several models have been used by other researchers to describe the sorption equilibria in WAC chelating and non-chelating resins [35,36]. The mass action law and Sips models have been used in this study for simplicity. For all the equilibrium isotherm experiments sodium ion was the counter ion initially in the solid phase. More details about the isotherm models definition and derivation are provided in the supplementary data. The molar selectivity coefficient ($K^c_{A,B}$) resulting from the mass action law fitting for different ions and resins investigated is shown in the box plot Fig. 4. The Sips isotherm model parameters (K_s, n) are reported in the supplementary data Tables (S1 and S2).

Using the mass action law, the ions equivalent fraction (n^*_A) in the solid phase as a function of its concentration in the solution phase (c^*_A) was defined as follows:

$$n^*_A = 1 - \frac{-1 + \sqrt{1 + 4\dfrac{K'_{A,B} c^*_A}{(1 - c^*_A)^2}}}{2\dfrac{K'_{A,B} c^*_A}{(1 - c^*_A)^2}}$$

in the case of divalent/monovalent ion exchange $z_A = 2\,\&\,z_B = 1$

(3.1)

$$n^*_A = 1 - \frac{1}{1 + \dfrac{K'_{A,B} c^*_A}{1 - c^*_A}}$$

in the case of monovalent/monovalent ion exchange $z_A = z_B = 1$

(3.2)

For Langmuir-Freundlich (Sip isotherm), the ion equivalent fraction (Y) in the solid phase for both monovalent/monovalent and divalent/monovalent ion exchange was calculated as follows:

$$Y = \frac{X^n}{r^*_s + X^n(1 - r^*_s)}, \quad r^*_s = \frac{1}{1 + K_s c_o{}^n} \tag{3.3}$$

Where $c^*_i = z_i c_i / c_{tot}$ and $n^*_i = z_i n_i / n_m$, $z_A \& z_B$ are ionic valences, $K'_{A,B}$ is dimensionless selectivity coefficient, c_{tot} is total solution concentration, n_m maximum exchange capacity, $Y = q_e/q_0$ and $X = c_e/c_0$, c_e and q_e are ion concentrations in the solution and resin at equilibrium, respectively. X is the equivalent ion fraction in the solution, c_0 and q_0 are the initial solution concentration and the related equilibrium loading, respectively. K_s and exponent n are Sips isotherm constants.

2.5. Kinetics experiments

Kinetics experiments were done for both Ca^{2+} and Mg^{2+} using DOWEX Marathon MSC, Lewatit S 8227, Amberlite IRC747, and Amberlite IRC748 resins initially in Na^+ form. The experiments were done in triplicate at room temperature (approx. 22 °C). A 10 meqv/L solution of Ca^{2+} and Mg^{2+} was prepared, and a resin dose of 50 % theoretical removal was chosen. Similar to equilibrium experiments, 100 mL of the prepared solution was used in each experiment. Samples of 2 mL were taken during the experiment at different time intervals. The samples were filtered on 0.45 μm syringe filters, and the calcium and magnesium concentrations were determined afterwards. Finally, the fractional uptake of ions was calculated based on equation 1.12 as shown in the supplementary data. The fractional uptake vs time curves were correlated with a kinetic model explained in the supplementary data.

Table 2
Anaerobic groundwater ionic composition from the Oasen water treatment plant at Kamerik, the Netherlands. A similar cations composition solution was prepared to test multicomponent solution equilibrium and kinetics under aerobic conditions. (pH ≅ 7.20).

Cations	Concentration (mM)	Anions	Concentration (mM)	Heavy metals	Concentration (mM)
Ca^{2+}	2.91 ± 0.20	HCO_3^-	6.45 ± 0.50	Fe^{2+}	0.14 ± 0.05
Na^+	2.20 ± 0.30	Cl^-	2.70 ± 0.50	Mn^{2+}	0.01 ± 0.006
Mg^{2+}	0.70 ± 0.18	SO_4^{2-}	0.43 ± 0.06		
NH_4^+	0.18 ± 0.03	F^-	0.007 ± 0.001		
K^+	0.14 ± 0.001				

3. Results and discussion

3.1. Single component sorption equilibria

3.1.1. Effect of resin dose on ions removal

The effect of resin dose on the removal of NH_4^+, K^+, Mg^{2+}, and Ca^{2+} ions using Amberlite IRC747, Amberlite IRC748, Lewatit S8227, and DOWEX Marathon MSC resins initially in Na^+ form was investigated. Fig. 2 (a-d), shows a clear difference in the removal of monovalent (NH_4^+ and K^+) and divalent (Mg^{2+} and Ca^{2+}) ions. Almost 100% removal of Ca^{2+} and Mg^{2+} was achieved at approximately 100% resin dose (i.e., the stoichiometric value), except for Mg^{2+} in the case of DOWEX Marathon MSC (app. 200% resin dose). Complete removal of NH_4^+ and K^+ was not achieved even at a resin dose 10 times higher than the stoichiometric value for all resins studied. This behaviour is attributed to the differences in the resins' selectivity towards monovalent and divalent ions. The resin selectivity is known to depend on ionic valence, ion hydration radius, and functional groups of the resin [37]. Ions with higher ionic valence have a lower ionic hydration radius and hence exhibit stronger electrostatic interaction towards ion exchange resin functional groups.

This can be clearly seen in Fig. 2 a – d where calcium and magnesium (divalent ions) had a significantly higher removal percentage at 100% resin dose than ammonium and potassium (monovalent ions) for all resins investigated. For ammonium, WAC resins had an average of ≈ 46% removal which is lower than SAC resin DOWEX Marathon MSC with 55% removal. A similar trend was found for potassium, WAC resins had an average removal percentage of ≈ 44%, compared to DOWEX Marathon MSC at 58%. When further increasing the resin dose (up to 1000%), a removal plateau is reached where WAC resins still have less NH_4^+ and K^+ removal than SAC resin. WAC resins showed a higher magnesium removal at 100% resin dose (roughly 92%) than SAC resin DOWEX MSC (87%). SAC and WAC resins had a similar calcium removal of more than 90% at a 100% resin dose.

3.1.2. Sorption isotherms

The IEX regenerant in the investigated remineralization scheme must be rich with hardness ions (calcium and magnesium) while having as low as possible ammonium and potassium content. In the previous section, resin dose versus ions removal curve was shown for each resin. Yet, sorption isotherms can be used for the quantitative analysis of the resins selectivity towards different components in the recovered ion-exchange regenerant solution. Single component sorption isotherms were constructed to evaluate the selectivity of the chosen cation exchange resins (Na^+-form) towards, NH_4^+, K^+, Mg^{2+}, and Ca^{2+} ions. Fig. 3 (a-d) shows the resulting sorption isotherms of NH_4^+, K^+, Mg^{2+}, and Ca^{2+} ions using Amberlite IRC747, Amberlite IRC748 and Lewatit S8227 weakly acidic (WAC) resins and DOWEX Marathon MSC strongly acidic (SAC) resin initially in Na^+ form.

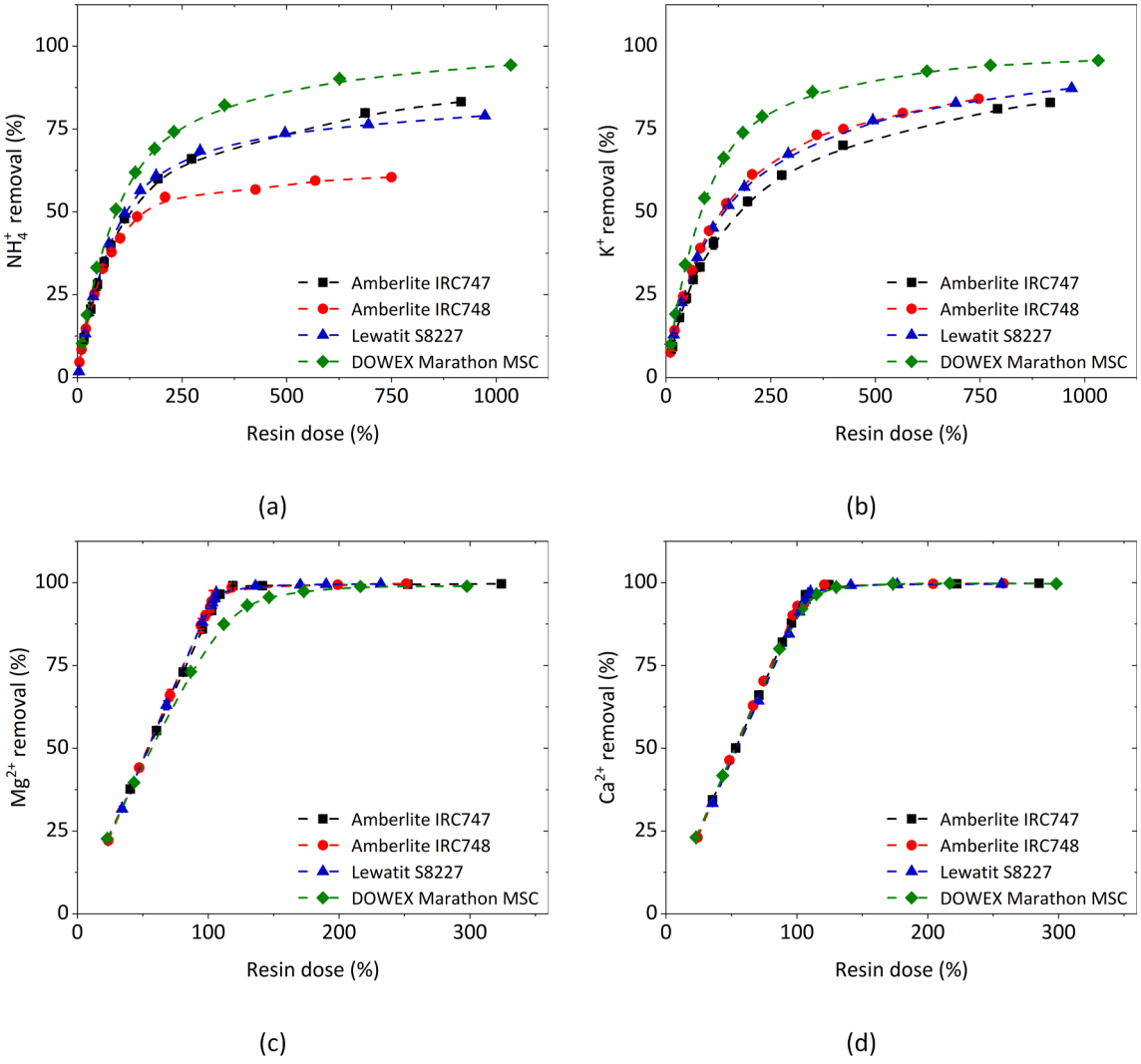

Fig. 2. Removal percentage at different resin doses for (a) NH_4^+, (b) K^+, (c) Mg^{2+}, and (d) Ca^{2+} on Amberlite IRC747, Amberlite IRC748, Lewatit S 8227, and DOWEX Marathon MSC resins respectively. Dashed lines are shown to guide the reader's eye.

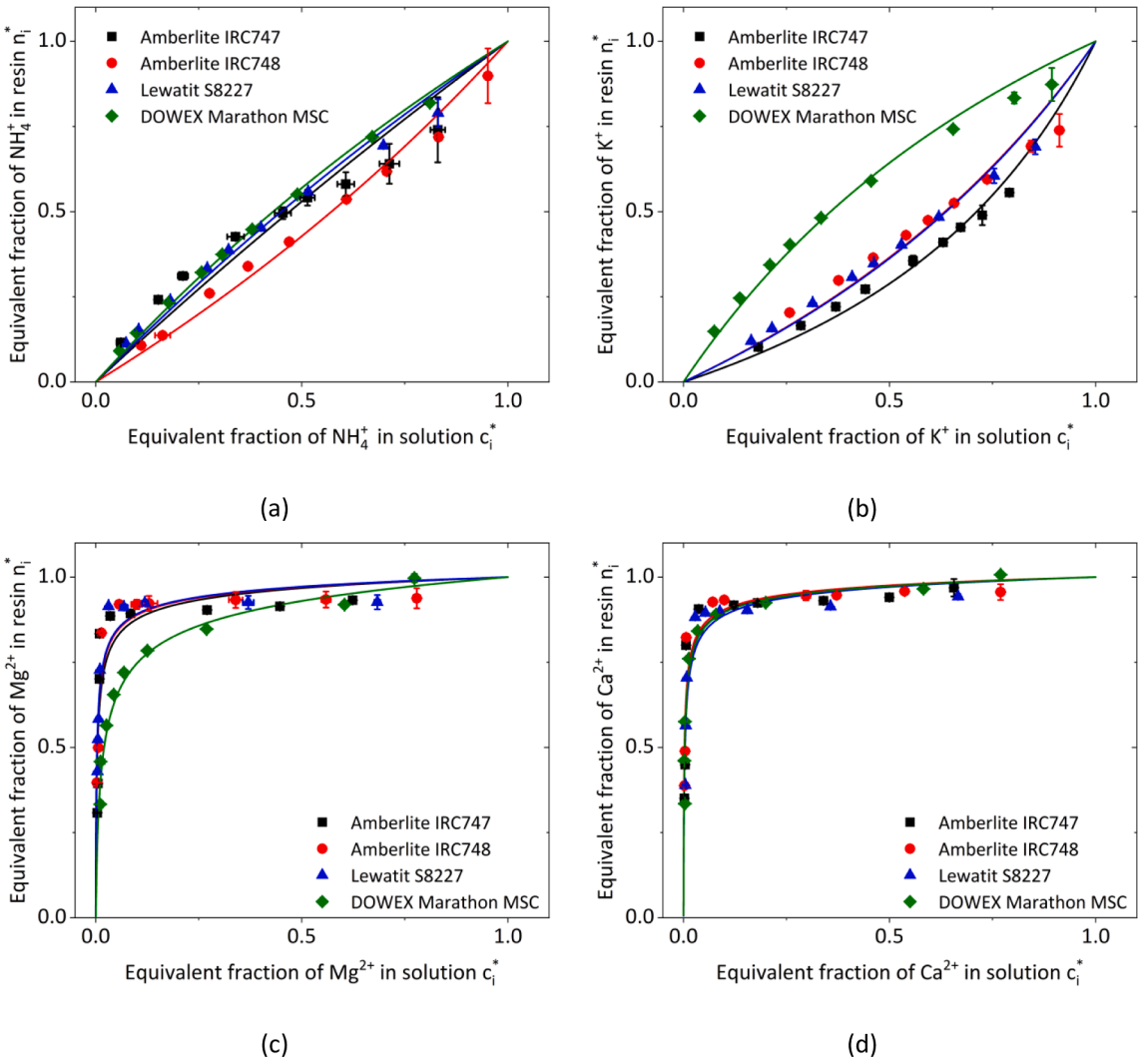

Fig. 3. Sorption isotherms for (a) NH_4^+, (b) K^+, (c) Mg^{2+}, and (d) Ca^{2+} on Amberlite IRC747, Amberlite IRC748, Lewatit S 8227, and DOWEX Marathon MSC resins respectively. The continuous lines represent the mass action law fitting of the sorption data.

The resin maximum exchange capacity (n_m) obtained by fitting calcium and magnesium sorption data using the mass action law and Sips isotherm was used in the calculation of the ions equivalent fraction in the resin (n_A^*, Y) in the dimensionless model instead of the total exchange capacity. n_m is slightly lower than the total exchange capacity and is dependent on the experimental conditions. Not all ion exchange sites are accessible for the ion exchange process due to blockage of larger ions by molecular sieve mechanism or being located in an inaccessible area in the polymer matrix. Moreover, ion exchange is an equilibrium reaction, therefore, a complete exhaustion of the resin's total capacity is only possible when the resin is contacted with a large excess of counter-ions. This was not the case in the investigated sorption experiments.

The mass action law model (Fig. 3 a – d) and Sips model (supplementary data **Fig. S1, Tables S1 and S2**) fit the sorption isotherm experimental data well. Data points corresponding to low resin dose (high equivalent ion fraction in solution) had the highest variability and therefore the experimental data show somewhat lower values than expected. The Sips model shows a slightly better fitting for both calcium and magnesium, especially at low ionic fraction compared to the mass action law fitting. On the other hand, monovalent ions were better fitted with the mass action law. It is noteworthy that the mass action law has only a single adjustable parameter for each binary system whereas the Sips isotherm has two. Therefore, the comparison of resins in terms of selectivity is here based on the mass action law model.

In Fig. 4, the values of the estimated molar selectivity coefficients clearly show the selectivity for calcium and magnesium over ammonium and potassium for all resins investigated. This result was expected because the resins prefer ions with higher valence (charge). However, when comparing ions with similar charge, the resins studied vary in their selectivity, especially in the case of monovalent ions. Amberlite IRC748 shows unfavourable sorption for ammonium, whereas other resins were slightly favourable. For potassium, only Marathon MSC shows favourable selectivity compared to the WAC resins. In contrast, Marathon MSC showed less favourable selectivity for magnesium than other resins. All resins showed significant selectivity for calcium even at a low solution ionic fraction.

The selectivity series for each ion according to the calculated molar selectivity coefficient using the mass action law model (Fig. 4) was as follows:

- NH_4^+ DOWEX Marathon MSC ≈ Lewatit S 8227 ≈ Amberlite IRC747 > Amberlite IRC748
- K^+ DOWEX Marathon MSC > Lewatit S 8227 ≈ Amberlite IRC748 ≈ Amberlite IRC747
- Mg^{2+} Amberlite IRC748 ≈ Amberlite IRC747 ≈ Lewatit S 8227 > DOWEX Marathon MSC
- Ca^{2+} Amberlite IRC748 ≈ Amberlite IRC747 ≈ DOWEX Marathon MSC ≈ Lewatit S 8227

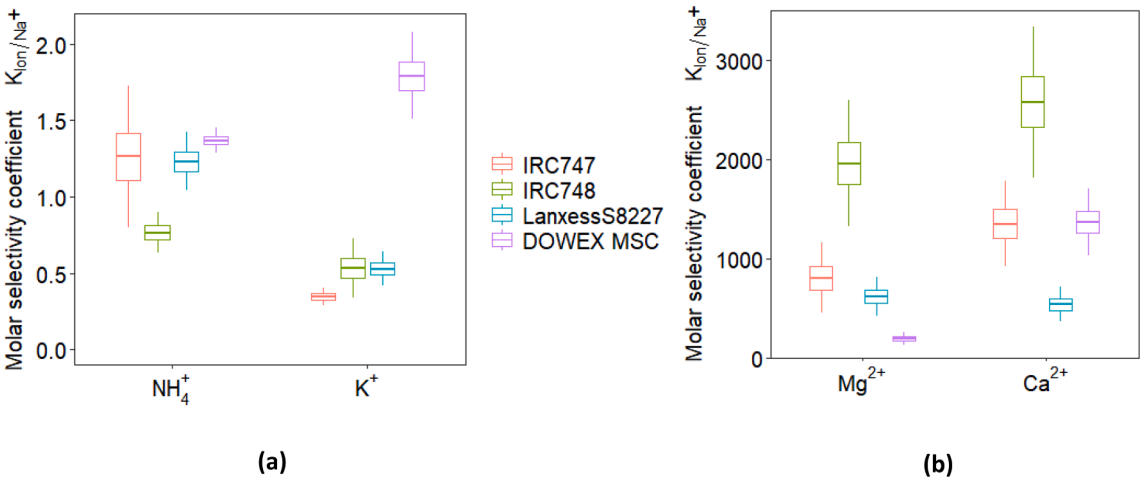

Fig. 4. Box plot shows the average calculated mass action law fitting parameter molar selectivity coefficient $K^{c}_{ion/Na}$ where the interquartile is ± 1 the standard error and the minimum and maximum values is ± 3 the standard error. Amberlite IRC748 chelating WAC resin has the highest selectivity for both b) divalent ions, while WAC resins have low selectivity for a) monovalent ions in where Amberlite IRC748 had the lowest selectivity for ammonium.

From a selectivity perspective, it can be concluded that Amberlite IRC748 WAC chelating resin is the most suitable resin to be used in the remineralization process presented previously since it has the lowest selectivity for ammonium and the highest for calcium and magnesium, which are the remineralization process requirements.

3.1.3. Discussion

The type of resin functional group, its degree of protonation and charge density carried play a significant role in resin selectivity towards the ions investigated. Fig. 5 shows the chemical structure of the functional groups attached to the studied resins polymeric matrix. Amberlite IRC747 and IRC748 are weakly acidic chelating resins with aminophosphonic and iminodiacetic acids functional groups, respectively [28,38]. Lewatit S8227 is an ordinary (non-chelating) weakly acidic resin with a carboxylic acid functional group on basis of crosslinked polyacrylate acid [39]. DOWEX Marathon MSC is a strongly acidic resin with a sulfonic acid group. In principle, ion exchange functional groups exhibit electrostatic coulombic interaction towards ions [37]. However, some resins, WAC resins, in particular, can have other interactions with ions next to the electrostatic interaction that can affect negatively or positively the selectivity towards different ions. In the case of Lewatit S8227, a carboxylic acid group in presence of hydrogen participate in a Brønsted Lowry acid-base reaction [40]. Moreover, for chelating resins, Amberlite IRC 747 and 748 with aminophosphonic and iminodiacetic acids functional groups can provide an ion pair to form ligand coordination bonding in a Lewis acid-base interaction [41]. This explains the high selectivity of WAC resins towards divalent ions which can form such bonding and have stronger interaction with the resin functional group.

The high selectivity of WAC resins for calcium and magnesium compared to SAC resin can be further explained using the charge separation distance theory [42]. SAC resins of a sulfonic group (DOWEX Marathon MSC) have less charge density (wet capacity) of functional groups per unit volume (2.51 ± 0.17 meqv/g) than WAC Lewatit S8227 (4.26 ± 0.01 meqv/g) as can be seen in Table 1, i.e. more distance between neighbouring ion-exchange sites than the carboxylic acid functional group in the WAC Lewatit S8227 resin [43]. As the charge density increases, a shorter distance between the ion exchange groups develops, which means, that a divalent ion with two charges forms a more stable bonding, with less work and hence higher selectivity. Furthermore, the specific interaction between the sulphonic group of the strongly acidic cation exchange resin DOWEX MARATHON MSC and calcium would be limited by the low solubility of $CaSO_3$ (0.054 g/L at 25 °C [44]). This means that the sulphonic group will act as a sink for calcium ions and hence the resin selectivity towards calcium would be limited.

The variation in NH_4^+ selectivity/removal between the resins studied is strongly related to the ability of weakly acid-fixed groups to participate in protonation/deprotonation reactions. The generated hydroxyl ions in this reaction are eliminated from the resin due to Donnan exclusion. Therefore, the pH inside the cation exchange resin decreases while the pH in the equilibrium solution increases and hence shifting the equilibrium from NH_4^+ to $NH_{3(aq)}$ (Fig. 6 a and b) [45]. The ability of the resin charged fixed groups to participate in the protonation-deprotonation reaction is determined by the pKa value, i.e., the concentration of the ionised H^+ ions at equilibrium in the solution. However, the amount of hydroxyl ions excluded is more dependent on the concentration of fixed charges in the resin i.e., the resin capacity. Despite that the wet capacity of the tested weakly acidic resins is varied (Lewatit S8227 = 4.26 ± 0.01 meqv/g, Amberlite IRC747 = 2.11 ± 0.05 meqv/g, and Amberlite IRC748 = 1.61 ± 0.01 meqv/g), the recorded pH at equilibrium in the bulk for NH_4^+ sorption seems to be similar for the three WAC resins investigated (Fig. 6a). Table 3 shows the pKa values of the functional groups of Amberlite IRC747 [46], Amberlite IRC748 [47 48] and Lewatit S8227 [49] resins. Chelating resins have

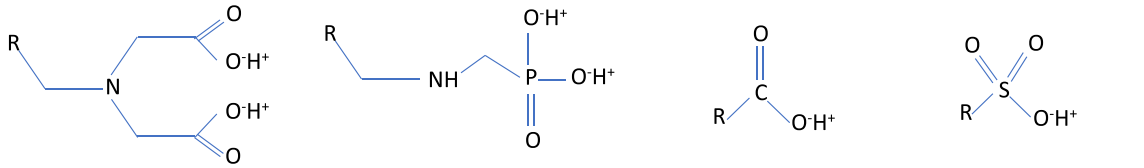

Amberlite IRC748 Iminodiacetic acid | Amberlite IRC747 Aminophosphonic acid | Lewatit S8227 carboxylic acid | DOWEX Marathon MSC Sulfonic acid

Fig. 5. Functional group chemical structure for chelating weakly acidic resins (Amberlite IRC748 & IRC747), non-chelating weakly acidic (Lewatit S8227) and strongly acidic (DOWEX Marathon MSC) resins studied.

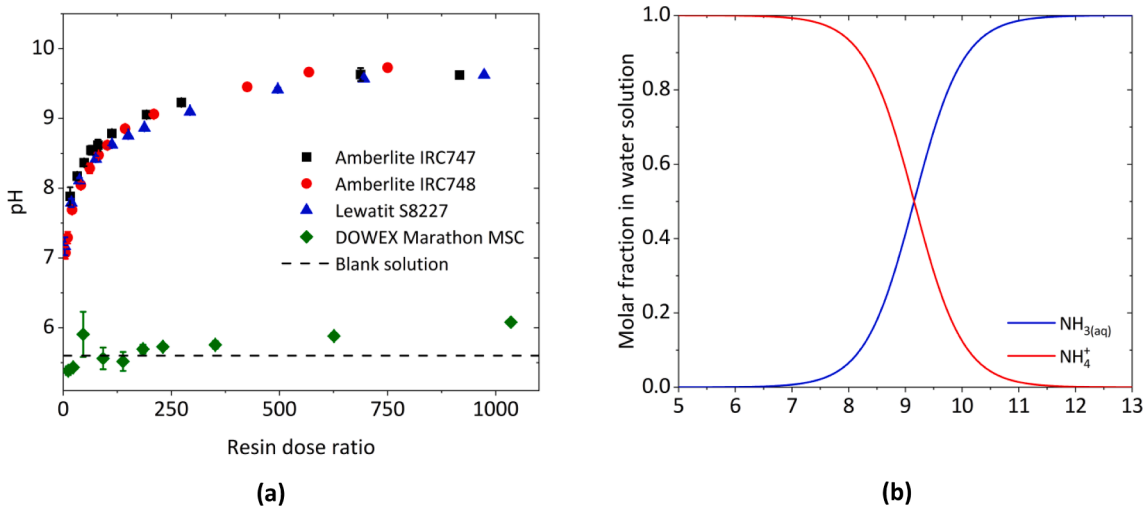

Fig. 6. A) The increase in bulk solution pH due to the increase in the amount of the resin used, i.e., the amount of fixed resin charges due to the exclusion of hydroxyl ions during WAC resins protonation-deprotonation reactions. Initial solution pH = 5.6. **b)** Ammonium/Ammonia equilibrium in water at 25 °C calculated according to equations proposed by Emerson et al. (1975) [52]. Continuous lines are shown to guide the reader's eye.

Table 3
Weakly acidic resins functional groups pKa values [46–49].

Resin	Functional group	pKa
Amberlite IRC747	Aminophosphonic acid	$pKa_1 = 0.5 – 1.5$ $pKa_2 = 5 – 6$ $pKa_3 = 9.5 – 10.5$
Amberlite IRC748	Iminodiacetic acid	$pKa_1 = 1.73$ $pKa_2 = 2.73$ $pKa_3 = 9.89$
Lewatit S 8227	Carboxylic acid	4.5

multiple pKa values compared to ordinary WAC ones due to the protonation potential of the N atom in the amine group [41,50].

Furthermore, WAC resins preferential sorption towards protons than NH_4^+ can be a reason behind the WAC resin low selectivity for NH_4^+. This phenomenon was also seen in anion exchange resins where NH_3 forms inside the resin functional group as its internal solution pH is shifted to the alkaline region compared to the external solution pH [51]. The increase in the internal pH shifts the equilibrium from NH_4^+ towards uncharged $NH_{3(aq)}$ (Fig. 6**b**), resulting in less NH_4^+ removal and hence less selectivity (Fig. 2**a** & 3**a**). The percentage of un-ionized ammonia based on pH and temperature was calculated according to equations proposed in literature [52,53]. Later the remaining NH_4^+ concentration was determined by subtracting the estimated $NH_{3(aq)}$ concentration from the total ammonium content measured by ion chromatography.

Amberlite IRC748 shows a much lower selectivity to ammonium compared to the other WAC resin as can be seen in Fig. 4a. This can be explained by looking at the resin charge density. Amberlite IRC748 has the lowest charge density (1.61 ± 0.01 meqv/g) compared to the other WAC resins Amberlite IRC747 and Lewatit S8227 (4.26 ± 0.01 and 2.11 ± 0.05, respectively). The lower the charge density the lower the resin selectivity towards the ion in the solution phase.

The sorption isotherms of the potassium using WAC resin are similar to the sorption isotherms of ammonium. This can also be attributed to the fact that WAC resins are more likely to participate in protonation-deprotonation reactions, the exclusion of hydroxyl ions by Donnan exclusion and the resin preferential sorption of protons. This implies less selectivity resin selectivity for both potassium and ammonium as explained earlier.

Amberlite IRC748 was used further in the remineralization process since it showed the lowest selectivity towards ammonium and the highest for calcium and magnesium, which complies with the selection criteria defined earlier for an efficient remineralization process. Low ammonium uptake is critical to the remineralization process to maintain a low ammonium content in the drinking water stream and ergo cause less bacterial growth potential [54].

3.2. Multi-component sorption equilibrium

The sorption equilibrium of a multi-component system using Amberlite IRC748 (Na^+ form) with a similar composition to the groundwater of Kamerik, the Netherlands (Table 2) was investigated. A synthetic solution of 2.35, 0.14, 0.16, 0.61, 2.83 mM of Na^+, NH_4^+, K^+, Mg^{2+}, and Ca^{2+} respectively was prepared and tested in aerobic conditions. The multicomponent solution was then contacted with different resin doses and the removal graph was made (Fig. 7). Although sodium background seems to be high in the model solutions. Its effect is not shown in Fig. 7, since the Amberlite IRC748 is initially in the Na^+ form and hence no removal is expected. Sodium concentration can only affect

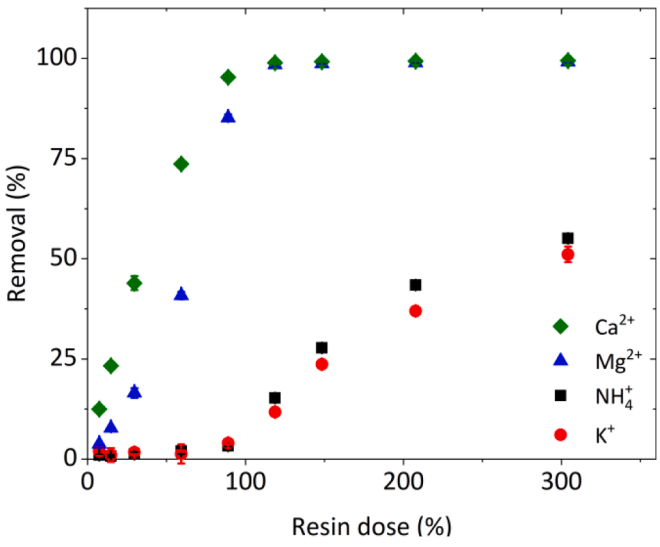

Fig. 7. The removal vs resin dose percentage of multicomponent system composed of NH_4^+, K^+, Mg^{2+}, and Ca^{2+} ions with similar concentrations as a real anaerobic groundwater sample provided by Oasen drink water company (Kamerik, the Netherlands) using Amberlite IRC748 in the Na^+ form. The experiment was done under aerobic conditions.

the total solution ionic strength, yet the model solution is dilute and hence the sorption of other ions forming the model solution is less affected by the sodium ion.

Fig. 7 shows that Amberlite IRC748 removed calcium the most followed by magnesium, ammonium and potassium. At 100 % resin dose, calcium removal was ~ 97%, magnesium 92%, and ~ 6% removal was observed for both ammonium and potassium. In the absence of divalent ions, Amberlite IRC748 shows a similar removal percentage of ammonium and potassium (55% at 300% resin dose) to the single component case shown earlier (Fig. 2 (a & b)). In a single-component system, Amberlite IRC748 showed the lowest selectivity for ammonium compared to other resins tested, however, in the multicomponent system (mixture) the resin selectivity appears to be entirely dominated by the presence of the divalent ions as can be seen in Fig. 7. Divalent ions were selectively removed in favour of the monovalent ions present.

3.3. Mass transfer kinetics

The mass transfer kinetics of calcium and magnesium ions using Amberlite IRC747, Amberlite IRC748, Lewatit S8227 and DOWEX Marathon MSC resins were studied. A resin dose of 50% theoretical removal was used to avoid ending up at very low concentrations at equilibrium and hence to improve the kinetic curve fitting accuracy. The resin was contacted with 0.01 M initial calcium and magnesium salt concentrations in batch experiments. The experiments continued until no further changes in solution concentration were noticed. Later, the fractional uptake vs time curves were constructed, and the exchange kinetics were investigated to assess the limiting transport step in the ion exchange process. Two main mass transfer limitations were defined: film diffusion and intraparticle diffusion.

3.3.1. Effect of magnetic stirrer mixing speed

Amberlite IRC747 was used for the investigation of solution mixing speed induced by a magnetic stirrer rotating at 180, 400, 600, and 800 rpms (Fig. 8). The Amberlite IRC748, Lewatit S8227 and DOWEX Marathon MSC resins were only tested in laminar (180 rpms) and transitional (800 rpms) regimes (Supplementary data – Fig. (S2)). Magnetic stirring speeds were chosen to test both laminar and transitional mixing regimes. The Reynolds number for each rotation speed was calculated according to Halász et al. (2007) [55] and shown in Table 4. More details about the Reynolds calculation and flask/stirrer bar size can be found in the supplementary data. A flow with a Reynolds number

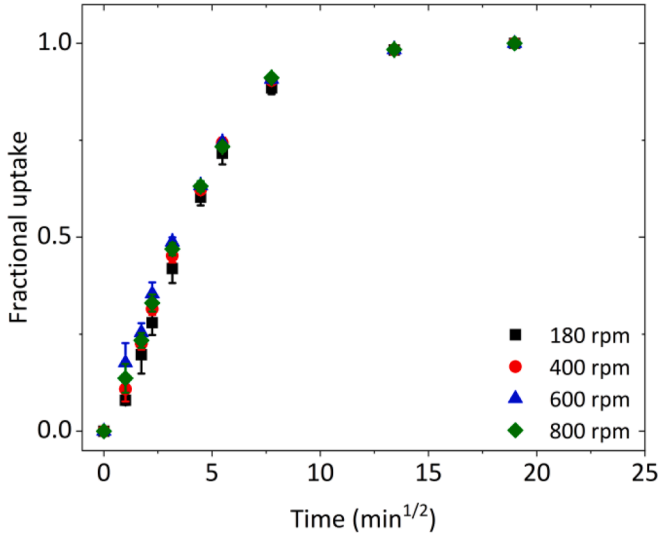

Fig. 8. Effect of stirrer rotation speed (rpms) on calcium fractional uptake in time ($min^{1/2}$) using Amberlite IRC747. Experiment done at room temperature (22 °C), C_0 = 10 meqv/L, m_w = 0.34 g and V_0 = 100 mL.

Table 4
Calculated Reynolds number as a function of magnetic stirring speed in rpms for single component batch kinetics experiments using 0.01 eqv/L calcium on Amberlite IRC747 resin.

Stirring speed (rpm)	Reynolds number
180	938
400	2077
600	3115
800	4154

less than ~ 10 to ~ 50 is considered laminar and a flow with more than 10,000 is turbulent, in between is a transitional flow regime [56,57]. The mixing speed is supposed to affect the thickness of the film boundary layer developed around the resin bead. However, Fig. 8 shows that calcium fractional uptake was independent of the mixing speed induced by the magnetic stirrer rotation. Based on this, the mass transfer in Amberlite IRC747 is unlikely film diffusion-controlled but rather intraparticle diffusion controlled. Similar findings were obtained for the other resins investigated (Supplementary data – Fig. (S2)).

3.3.2. Mass transfer diffusion limitation

The mass transfer kinetics for both calcium and magnesium for the different studied resins were investigated. Fig. 9 a & b shows the experimental data as fractional uptake. The kinetic data were correlated using an intraparticle diffusion model based on the Nernst-Planck equation (equations (3.4) to (3.7)). Similar relationships have been used by Yoshida et al. (1985) [58] and Valverde et al. (2005) [59].

The resin particles were assumed to be spherical. The mean particle size was used in the model and the size distribution was not considered. Diffusion was assumed to occur in a (pseudo) homogeneous medium even though some of the materials were macroporous. The principle of electroneutrality applies and hence the summation of electric current equals zero everywhere.

$$\sum_j z_j J_j = 0 \tag{3.4}$$

where z_j is ionic valence and J_j is the diffusion flux (mol/m^2/s) of species j.

In absence of an external electric field, the flux is calculated using the Nernst-Planck equation as:

$$J_j = -D_j\left(\frac{\partial q_j}{\partial r} + z_j q_j \frac{F}{RT}\frac{\partial \varphi}{\partial r}\right) \tag{3.5}$$

where D_j is diffusion coefficient (m^2/s) of the jth ion, q_j is the local concentration of the ion in the resin particle (mol/kg), r is radial coordinate (m), z_j is the ion valence, F is Faraday's constant = 96485.33 (C/mol), R is gas constant = 8.314 ($J.K^{-1}.mol^{-1}$), and T is the temperature (K).

The fluxes of different species are not independent but linked to each other through the gradient in local electric potential ($\frac{\partial \varphi}{\partial r}$) in the particle and the electroneutrality/zero current requirement, which is given by Eqn. (3.6).

$$\frac{\partial \varphi}{\partial r} = -\frac{RT\sum_j z_j D_j \frac{\partial q_j}{\partial r}}{F\sum_j z^2{}_j D_j q_j} \tag{3.6}$$

When the fluxes are solved from Eqs. (3.4) to (3.6), the change in local concentration is calculated from the differential material balance for diffusion in a sphere.

$$\frac{\partial q_j}{\partial t} = -\frac{1}{r^2}\frac{\partial}{\partial r}\left(r^2 J_j\right) \tag{3.7}$$

More details about the intraparticle diffusion model can be found in the supplementary data.

All fractional uptake curves except that for DOWEX MARATHON

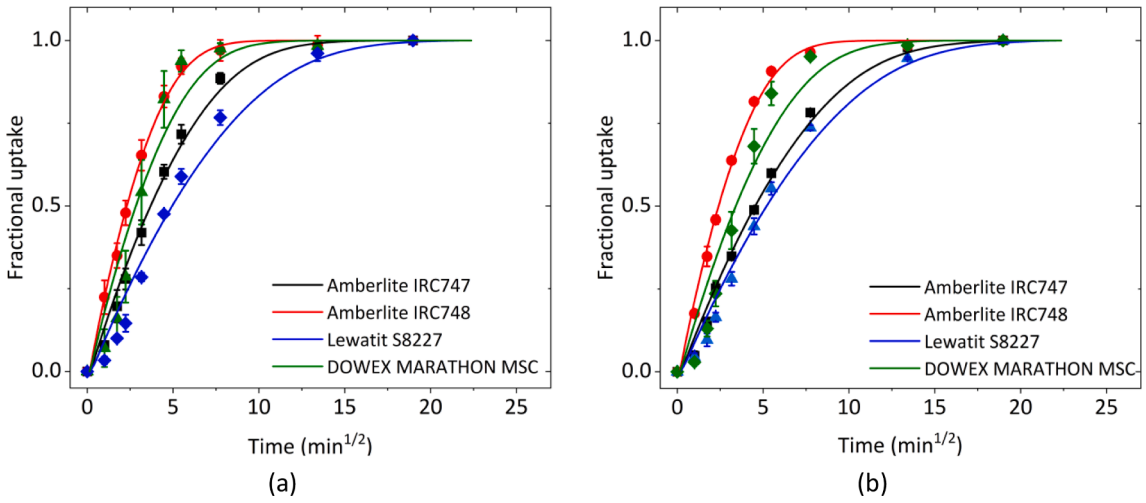

Fig. 9. Ion exchange single component kinetics using 0.01 M a) calcium and b) magnesium concentration in the batch experiment. The resin fraction uptake was fitted (connected line) using intraparticle mass transfer diffusion model based on Nernst-Planck equation.

MSC could be fitted quite well with the intraparticle diffusion model. Fig. 9 a & b show a similar fractional uptake behaviour of the resins tested for both calcium and magnesium. The experimental data in Fig. 9 a & b clearly show that Amberlite IRC748 had the fastest kinetics followed by DOWEX MARATHON MSC, Amberlite IRC747 and Lewatit S8227, respectively for both calcium and magnesium. This observation matches the calculated intraparticle mass transfer coefficient shown in Table 5, where Amberlite IRC748 had the fastest diffusion coefficient for both calcium ($8.65 \pm 0.58 \times 10^{-12}$ m^2/s) and magnesium (7.95 ± 0.38x 10^{-12} m^2/s). The calcium and magnesium intraparticle diffusion coefficient reported is a little bit smaller than what is reported by other researchers [59]. This is mainly due to the assumption that has been made in the model. The mass transfer area is overestimated by 1/resin porosity since diffusion is assumed to occur in a homogeneous material. Furthermore, the ions distance travelled is underestimated given pores tortuosity was neglected. In addition, the resin surface area is underestimated since average particle diameter is used where resin has a size distribution. All these factors affect the estimated ion diffusion coefficients.

The variation in uptake rate can be attributed to several factors discussed by Helfferich (1962) [37], including resin particle size and the nature of the functional group and the selectivity of ion exchanger. The observed uptake rate is inversely proportional to particle size squared. By reducing the resin bead size, the time required to attain equilibrium is significantly reduced and hence faster mass transfer kinetics are achieved. Furthermore, the intraparticle diffusion is slower for resins with functional groups that associate with counter ions as, for instance, chelating resins (Amberlite IRC747 & 748) forming Lewis-base interaction with counterions. In addition, the preferred ion would be taken up at a faster rate and released at a slower rate which would result in slower mass transfer kinetics.

Fig. 9 shows that Lewatit S8227 has the slowest fractional uptake in the case of calcium as well as magnesium, while Amberlite IRC748 and DOWEXMSC are the fastest. This observation can be purely attributed to the variation in particle size shown in Table 1. The mean particle diameter of Lewatit S8227 (780 ± 15 μm) is higher than that of Amberlite IRC748 and DOWEX MARATHON MSC (578 ± 5 and 565 ± 1 μm) respectively. The diffusion time is proportionally dependent on the particle diameter squared, and hence a shorter ion diffusion time is achieved with a lower particle diameter. The resins particle size distribution is provided in the supplementary data (Fig. S3). The effect of the resin functional group or the resin selectivity on the calcium or magnesium mass transfer rate can be seen for DOWEX MARATHON MSC and Amberlite IRC 747. The chelating resin Amberlite IRC 747 has a slower uptake than the non-chelating DOWEX MARATHON MSC. The higher diffusion coefficient of Amberlite IRC748 may stem from its macropore size distribution or swelling of the polymer network, but these could not be quantified here.

Table 5
Intraparticle mass transfer coefficient (K_s) and 95% confidence intervals for calcium and magnesium kinetics using the studied resins. Calcium or magnesium initial concentration = 0.01 M, stirring speed = 180 rpm.

Resin	Calcium (10^{-12} m^2/s)	Magnesium (10^{-12} m^2/s)
Amberlite IRC747	3.40 ± 0.32	2.25 ± 0.17
Amberlite IRC748	8.65 ± 0.58	7.95 ± 0.38
Lewatit S8227	3.40 ± 0.53	3.08 ± 0.39
DOWEX MARATHON MSC	5.45 ±1.3	3.78 ± 0.80

3.3.3. *Multi-component kinetics*

A mixture of similar composition to the groundwater characteristics shown in Table 2 was prepared and the mass transfer kinetics using

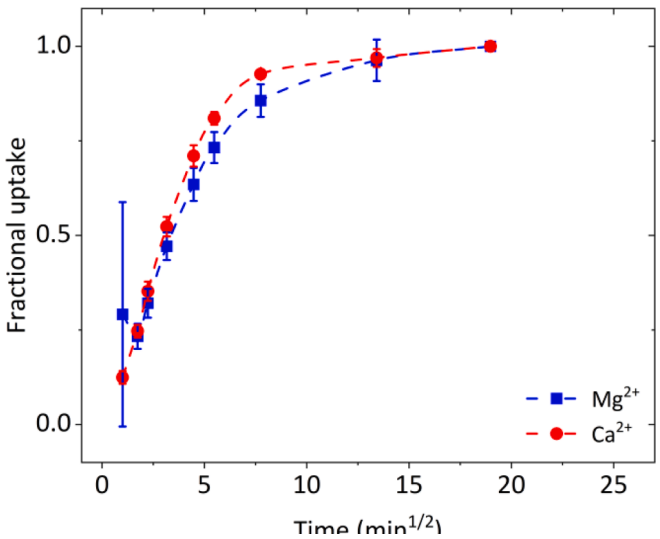

Fig. 10. The fractional uptake of Mg^{2+}, and Ca^{2+} ions as part of a multicomponent system with a similar composition to groundwater in Kamerik, the Netherlands using Amberlite IRC748 in the Na^+ form. High error bar at initial Mg^{2+} fractional uptake might be due to an outlier measurement. Dashed lines are shown to guide the reader's eye.

Amberlite IRC748 resin (Na^+ form) was determined. Fig. 10 shows the resin fractional uptake of calcium and magnesium as a function of time. As has been shown earlier in Fig. 7, at a resin dose of less than 100 %, divalent ions dominate the Amberlite IRC748 resin selectivity and hence the resin selectivity for monovalent ions such as ammonium and potassium is negligible. The resin dose used in the mixture kinetic experiment was 50% and, therefore, the ammonium and potassium were hardly removed. Their fractional uptake (5.0% at maximum) is therefore not shown in Fig. 10. In a mixture, calcium and magnesium show quite similar mass transfer kinetics (Fig. 10), which was also the case when their mass transfer kinetics were tested individually (Fig. 9 a&b). This similarity in fractional uptake can be attributed to their nearly identical diffusion coefficients and hydrated radii. The magnesium ionic hydrated radius (4.28 Å [60]) is slightly higher than calcium (4.12 Å) and their intraparticle diffusivities are shown in Table 5.

4. Conclusions

An ion exchange resin – bipolar membrane electrodialysis hybrid process was designed for sustainable reverse osmosis permeate remineralization. The remineralization process is necessary to increase the RO permeate buffering capacity and mineral content, in particular, hardness to comply with legal and guidelines requirements. Equilibria and kinetics of selected cation exchange resins were investigated to select the most promising resin based on defined remineralization criteria. The selected resin must have a high selectivity for calcium and magnesium and a low selectivity for ammonium and potassium. Furthermore, high mass transfer kinetics are desirable to achieve regeneration in a reasonable time.

Cation exchange resins with different functional groups including chelating WAC resins (Amberlite IRC747 and IRC748), a non-chelating WAC resin (Lewatit S8227) and a SAC resin (DOWEX MARATHON MSC) were selected. In single-component equilibrium experiments, the selected resins varied significantly in their selectivity towards monovalent (NH_4^+, K^+) and divalent (Mg^{2+} and Ca^{2+}) ions. Generally speaking, all ion exchange resins investigated showed higher selectivity for ions with higher ionic valence, whereas WAC resins exhibited less selectivity and removal towards monovalent ions compared to SAC resin DOWEX MARATHON MSC. Amberlite IRC748 showed an exceptionally low removal (max 60%) and selectivity ($K^c_{NH4/Na}^+ = 0.77 \pm 0.19$) for ammonium compared to other WAC resins tested given low charge density. However, in a multi-component system, the selectivity of the Amberlite IRC748 resin was completely dominated by the presence of the divalent ions calcium and magnesium, which is well known effect considering the Donnan equilibrium theory where ions with higher valence are sorbed preferentially. Therefore, all WAC resins tested are expected to behave similarly in a multi-component system where the selectivity for divalent ions prevails.

The mass transfer limitations in the cation exchange resins were investigated in both single and multi-component kinetics batch experiments. Cation exchange resins showed a similar fractional uptake under laminar and transitional flow regimes, therefore, the ions mass transfer limitation is unlikely film diffusion-controlled, but rather intraparticle diffusion-controlled, since any boundary layer around a film would reduce in size with higher flow rates/stirring speeds. A mass transfer intraparticle kinetics model based on the Nernst-Planck equation was used to fit the fractional uptake curves of the ion exchange resins. Amberlite IRC748 had the fastest diffusion coefficient for both calcium ($8.65 \pm 0.58 \times 10^{-12}\ m^2/s$) and magnesium ($7.95 \pm 0.38 \times 10^{-12}\ m^2/s$) compared to other reins investigated. Calcium and magnesium intraparticle mass transfer diffusion kinetics were quite similar in both single and multi-component systems.

Out of the resins investigated, Amberlite IRC748 is recommended to be used in the investigated remineralization process, although it showed similar selectivity towards divalent and monovalent ions to other WAC resins investigated in a multi-component system. Yet, based on single component sorption, Amberlite IRC748 had high selectivity for both calcium and magnesium and low selectivity for ammonium and potassium, which matches the remineralization process criteria defined earlier. Furthermore, Amberlite IRC748 did show superior mass transfer diffusion kinetics compared to the other resins investigated. Using Amberlite IRC748 in the remineralization process will allow RO to operate at high recoveries due to less scaling potential due to the divalent ions absence. Furthermore, the recovered regenerant stream will be rich with hardness ions required for RO permeate remineralization.

CRediT authorship contribution statement

A.A.M. Abusultan: Methodology, Conceptualization, Investigation, Writing – original draft. **J.A. Wood:** Supervision, Writing – review & editing. **T. Sainio:** Writing – review & editing. **A.J.B. Kemperman:** Supervision, Writing – review & editing. **W.G.J. van der Meer:** Supervision, Writing – review & editing.

Declaration of Competing Interest

The authors declare the following financial interests/personal relationships which may be considered as potential competing interests: Almohanad Abusultan reports financial support was provided by Oasen NV. Walter van der Meer reports a relationship with Oasen NV that includes: board membership and employment. Walter van der Meer, Almohanad Abusultan has patent Method For Purifying Water As Well As Plant Suitable For Said Method issued to Oasen NV.

Data availability

Data will be made available on request.

Acknowledgements

This work was financially supported by Dutch water supply company OASEN N.V.

Appendix A. Supplementary data

Supplementary data to this article can be found online at https://doi.org/10.1016/j.seppur.2023.123798.

References

[1] M. Qasim, M. Badrelzaman, N.N. Darwish, N.A. Darwish, N. Hilal, Reverse osmosis desalination: A state-of-the-art review, Desalination 459 (2019) 59–104, https://doi.org/10.1016/j.desal.2019.02.008.
[2] Y. Pouliot, Membrane processes in dairy technology—From a simple idea to worldwide panacea, Int. Dairy J. 18 (7) (2008) 735–740, https://doi.org/10.1016/j.idairyj.2008.03.005.
[3] World Health Organization: Sustainable Development and Healthy Environments Cluster, *Nutrients in drinking water*. Geneva: World Health Organization, 2005.
[4] A. Withers, Options for recarbonation, remineralisation and disinfection for desalination plants, Desalination 179 (1) (2005) 11–24, https://doi.org/10.1016/j.desal.2004.11.051.
[5] J.A. Cotruvo, J. Bartram, *Calcium and Magnesium in Drinking-water: Public Health Significance*. World Health Organization, 2009. Available online: https://www.who.int/publications/i/item/9789241563550 (accessed 23-06-222).
[6] F. Kozisek, Regulations for calcium, magnesium or hardness in drinking water in the European Union member states, Regul. Toxicol. Pharm. 112 (2020), 104589, https://doi.org/10.1016/j.yrtph.2020.104589.
[7] *Drinkwaterbesluit*. Available online: https://wetten.overheid.nl/BWBR0030111/2021-10-13 (accessed, 20 October 2021).
[8] L. Birnhack, N. Voutchkov, O. Lahav, Fundamental chemistry and engineering aspects of post-treatment processes for desalinated water—A review, Desalination 273 (1) (2011) 6–22, https://doi.org/10.1016/j.desal.2010.11.011.
[9] W.G.J. Van der Meer, A.A.M. Abusultan, *Method For Purifying Water As Well As Plant Suitable For Said Method*. Patent application number: EP 18161272, 2018.
[10] C. van den Brink, Land use an groundwater quality: How technical instrumentation and scientific knowledge can support groundwater planning, De Hoog Grafische diensten BV, Utrecht, 2009.

[11] M.P. Sauvant, D. Pepin, Drinking water and cardiovascular disease, Food Chem. Toxicol. 40 (10) (2002) 1311–1325, https://doi.org/10.1016/S0278-6915(02)00081-9.

[12] S. Marque, H. Jacqmin-Gadda, J.-F. Dartigues, D. Commenges, Cardiovascular mortality and calcium and magnesium in drinking water: An ecological study in elderly people, Eur. J. Epidemiol. 18 (4) (2003) 305–309, https://doi.org/10.1023/A:1023618728056.

[13] J. Ferrándiz, J.J. Abellán, V. Gómez-Rubio, A. López-Quílez, P. Sanmartín, C. Abellán, M.A. Martínez-Beneito, I. Melchor, H. Vanaclocha, Ó. Zurriaga, F. Ballester, J.M. Gil, S. Pérez-Hoyos, R. Ocaña, Spatial Analysis of the Relationship between Mortality from Cardiovascular and Cerebrovascular Disease and Drinking Water Hardness, Environ. Health Perspect. 112 (9) (2004) 1037–1044, https://doi.org/10.1289/ehp.6737.

[14] M. Momeni, Z. Gharedaghi, M.M. Amin, P. Poursafa, M. Mansourian, Does water hardness have preventive effect on cardiovascular disease? Int. J. Prev. Med. 5 (2) (2014) 159–163. http://www.ncbi.nlm.nih.gov/pmc/articles/pmc3950737/.

[15] S.P. Allwright, A. Coulson, R. Detels, C.E. Porter, Mortality and water-hardness in three matched communities in Los Angeles, Lancet 2 (7885) (1974) 860–864, https://doi.org/10.1016/s0140-6736(74)91200-8.

[16] R.W. Morris, M. Walker, L.T. Lennon, A.G. Shaper, P.H. Whincup, Hard drinking water does not protect against cardiovascular disease: new evidence from the British Regional Heart Study, Eur. J. Cardiovasc. Prev. Rehabil. 15 (2) (2008) 185–189, https://doi.org/10.1097/hjr.0b013e3282f15fce.

[17] L.J. Leurs, L.J. Schouten, M.N. Mons, R.A. Goldbohm, P.A. van den Brandt, Relationship between tap water hardness, magnesium, and calcium concentration and mortality due to ischemic heart disease or stroke in The Netherlands, Environ. Health Perspect. 118 (3) (2010) 414–420, https://doi.org/10.1289/ehp.0900782.

[18] Kožíšek, F., *Health significance of drinking water calcium and magnesium.* National Institute of Public Health, 2003. **29**: p.9285-9286. Available online: http://www.szu.cz/uploads/documents/chzp/voda/pdf/hardness.pdf (accessed on 21 June 2022).

[19] R.E. Loewenthal, I. Morrison, M.C. Wentzel, Control of corrosion and aggression in drinking water systems, Water Sci. Technol. 49 (2) (2004) 9–18, https://doi.org/10.2166/wst.2004.0075.

[20] B.E. Rittmann, V.L. Snoeyink, Achieving Biologically Stable Drinking Water, J. AWWA 76 (10) (1984) 106–114, https://doi.org/10.1002/j.1551-8833.1984.tb05427.x.

[21] D. van der Kooij, W. Hijnen, Regrowth of bacteria on assimilable organic carbon in drinking water, J. français d'hydrologie 16 (1985) 201–218, https://doi.org/10.1051/water/19851603201.

[22] World Health Organization, Potassium in drinking-water: background document for development of WHO guidelines for drinking-water quality, World Health Organization, Geneva, 2009.

[23] M. Luqman, Ion Exchange Technology II: Applications, Springer, Netherlands, 2012. https://doi.org/10.1007/978-94-007-4026-6.

[24] S.J. Gerberding, C.H. Byers, Preparative ion-exchange chromatography of proteins from dairy whey, J. Chromatogr. A 808 (1) (1998) 141–151, https://doi.org/10.1016/S0021-9673(98)00103-4.

[25] Mohebbi, A., Abolghasemi Mahani, A., and Izadi, A., Ion exchange resin technology in recovery of precious and noble metals, in Applications of Ion Exchange Materials in Chemical and Food Industries, Inamuddin, T.A. Rangreez, and A. M. Asiri, Editors. 2019, Springer International Publishing: Cham. pp. 193-258. https://doi.org/10.1007/978-3-030-06085-5_9.

[26] H. Hoffmann, F. Martinola, Selective resins and special processes for softening water and solutions; A review, Reactive Polymers, Ion Exchangers, Sorbents 7 (2) (1988) 263–272, https://doi.org/10.1016/0167-6989(88)90148-1.

[27] R. Kunin, R.E. Barry, Carboxylic, Weak Acid Type, Cation Exchange Resin, Ind. Eng. Chem. 41 (6) (1949) 1269–1272, https://doi.org/10.1021/ie50474a028.

[28] Z. Zainol, M.J. Nicol, Comparative study of chelating ion exchange resins for the recovery of nickel and cobalt from laterite leach tailings, Hydrometall. 96 (4) (2009) 283–287, https://doi.org/10.1016/j.hydromet.2008.11.005.

[29] M.V. Dinu, E.S. Dragan, Heavy metals adsorption on some iminodiacetate chelating resins as a function of the adsorption parameters, React. Funct. Polym. 68 (9) (2008) 1346–1354, https://doi.org/10.1016/j.reactfunctpolym.2008.06.011.

[30] Rohm and Haas compnay, *MTM 0250: Total anion and cation exchange capacity: Amphoteric resins*, 2000.

[31] E. Worch, Adsorption Technology in Water Treatment: Fundamentals, Processes, and Modeling, De Gruyter, Berlin, Boston, 2012. https://doi.org/10.1515/9783110240238.

[32] Rohm and Haas compnay, *MTM 0100: Moisture Holding Capacity testing protocol*, 1998.

[33] Y. Hu, J. Foster, T.H. Boyer, Selectivity of bicarbonate-form anion exchange for drinking water contaminants: Influence of resin properties, Sep. Purif. Technol. 163 (Supplement C) (2016) 128–139, https://doi.org/10.1016/j.seppur.2016.02.030.

[34] R. Sips, On the Structure of a Catalyst Surface, J. Chem. Phys. 16 (5) (1948) 490–495, https://doi.org/10.1063/1.1746922.

[35] W.H. Höll, J. Horst, M. Wernet, Application of the surface complex formation model to exchange equilibria on ion exchange resins. Part II. Chelating resins, Reactive Polymers 14 (3) (1991) 251–261, https://doi.org/10.1016/0923-1137(91)90041-L.

[36] M. Pesavento, R. Biesuz, M. Gallorini, A. Profumo, Sorption mechanism of trace amounts of divalent metal ions on a chelating resin containing iminodiacetate groups, Anal. Chem. 65 (18) (1993) 2522–2527, https://doi.org/10.1021/ac00066a021.

[37] F.G. Helfferich, Ion Exchange, McGraw-Hill, New York, 1962.

[38] X. Hérès, V. Blet, P. Di Natale, A. Ouaattou, H. Mazouz, D. Dhiba, F. Cuer, Selective Extraction of Rare Earth Elements from Phosphoric Acid by Ion Exchange Resins, Metals 8 (9) (2018) 682, https://doi.org/10.3390/met8090682.

[39] V. Soldatov, S. Pristavko, V. Zelenkovskii, E. Kosandrovich, Hydration of ion exchangers: Thermodynamics and quantum chemistry calculations, React. Funct. Polym. 73 (5) (2013) 737–744, https://doi.org/10.1016/j.reactfunctpolym.2013.03.001.

[40] T. Akiyama, K. Mori, Stronger Brønsted Acids: Recent Progress, Chem. Rev. 115 (17) (2015) 9277–9306, https://doi.org/10.1021/acs.chemrev.5b00041.

[41] P. Myers, *How chelating resins behave.* Plating and surface finishing **85**(10) (1998) 22-29. Available online: https://www.nmfrc.org/pdf/9810022.pdf (Accessed 21 June 2022).

[42] S. Subramonian, D. Clifford, Monovalent/divalent selectivity and the charge separation concept, Reactive Polymers, Ion Exchangers, Sorbents 9 (2) (1988) 195–209, https://doi.org/10.1016/0167-6989(88)90033-5.

[43] A.K. SenGupta, Ion exchange in environmental processes: Fundamentals, applications and sustainable technology, John Wiley & Sons, USA, 2017.

[44] W.M. Haynes, CRC Handbook of Chemistry and Physics, 97th ed., CRC Press, United states, 2016. https://doi.org/10.1201/9781315380476.

[45] N. Pismenskaya, V. Sarapulova, A. Klevtsova, S. Mikhaylin, L. Bazinet, Adsorption of Anthocyanins by Cation and Anion Exchange Resins with Aromatic and Aliphatic Polymer Matrices, Int. J. Mol. Sci. 21 (21) (2020) 7874.

[46] D. Villemin, M.A. Didi, Aminomethylenephosphonic acids syntheses and applications (A Review), Orient. J. Chem. 31 (2015) 1–12. https://doi.org/10.13005/ojc/31.Special-Issue1.01.

[47] A. Bossi, P.G. Righetti, Generation of peptide maps by capillary zone electrophoresis in isoelectric iminodiacetic acid, Electrophoresis 18 (11) (1997) 2012–2018, https://doi.org/10.1002/elps.1150181122.

[48] *National Center for Biotechnology Information, Iminodiacetic acid, CID=8897.* PubChem Database. Available online: https://pubchem.ncbi.nlm.nih.gov/compound/8897 (Accessed January 1, 2020).

[49] A.S. Michaels, O. Morelos, Polyelectrolyte Adsorption by Kaolinite, Ind. Eng. Chem. 47 (9) (1955) 1801–1809, https://doi.org/10.1021/ie50549a029.

[50] S. Procházková, V. Kubíček, Z. Böhmová, K. Holá, J. Kotek, P. Hermann, DOTA analogues with a phosphinate-iminodiacetate pendant arm: modification of the complex formation rate with a strongly chelating pendant, Dalton Trans. 46 (31) (2017) 10484–10497, https://doi.org/10.1039/C7DT01797A.

[51] E. Skolotneva, K. Tsygurina, S. Mareev, E. Melnikova, N. Pismenskaya, V. Nikonenko, High Diffusion Permeability of Anion-Exchange Membranes for Ammonium Chloride: Experiment and Modeling, Int. J. Mol. Sci. 23 (10) (2022) 5782.

[52] K. Emerson, R.C. Russo, R.E. Lund, R.V. Thurston, Aqueous Ammonia Equilibrium Calculations: Effect of pH and Temperature, J. Fish. Res. Board Can. 32 (12) (1975) 2379–2383, https://doi.org/10.1139/f75-274.

[53] A. Pano, E.J. Middlebrooks, Ammonia Nitrogen Removal in Facultative Wastewater Stabilization Ponds, Journal (Water Pollution Control Federation) 54 (4) (1982) 344–351. http://www.jstor.org/stable/25041312.

[54] M. Sousi, G. Liu, S.G. Salinas-Rodriguez, L. Chen, J. Dusseldorp, P. Wessels, J. C. Schippers, M.D. Kennedy, W. van der Meer, Multi-parametric assessment of biological stability of drinking water produced from groundwater: Reverse osmosis vs. conventional treatment, Water Res. 186 (2020), 116317, https://doi.org/10.1016/j.watres.2020.116317.

[55] G. Halász, B. Gyüre, I.M. Jánosi, K.G. Szabó, T. Tél, Vortex flow generated by a magnetic stirrer, Am. J. Phys 75 (12) (2007) 1092–1098, https://doi.org/10.1119/1.2772287.

[56] A.W. Nienow, Stirring and Stirred-Tank Reactors, Chem. Ing. Tech. 86 (12) (2014) 2063–2074, https://doi.org/10.1002/cite.201400087.

[57] D.W. Green, R.H. Perry, Perry's Chemical Engineers' Handbook, Eighth Edition, McGraw-Hill Education, United States, 2007. https://doi.org/10.1036/0071511245.

[58] H. Yoshida, T. Kataoka, S. Ikeda, Intraparticle mass transfer in bidispersed porous ion exchanger part I: Isotopic ion exchange, Can. J. Chem. Eng. 63 (3) (1985) 422–429, https://doi.org/10.1002/cjce.5450630310.

[59] J.L. Valverde, A. De Lucas, M. Carmona, M. González, J.F. Rodríguez, Model for the determination of diffusion coefficients of heterovalent ions in macroporous ion exchange resins by the zero-length column method, Chem. Eng. Sci. 60 (21) (2005) 5836–5844, https://doi.org/10.1016/j.ces.2005.05.043.

[60] J. Barthel, R. Jaenicke, B.E. Conway, Ionic Hydration in Chemistry and Biophysics.—Vol. 12 aus: Studies in Physical and Theoretical Chemistry. Elsevier Scientific Publishing Company, Amsterdam and New York 1981. 768 Seiten, Preis: £131.75. Berichte der Bunsengesellschaft für physikalische Chemie 86(3) (1982) 264-264. https://doi.org/10.1002/bbpc.19820860319.